

# Chapter 13

## Analysis of the Contamination Process of the Extremely Contaminated Fat Greenling by Fukushima-Derived Radioactive Material

Tomowo Watanabe, Ken Fujimoto, Yuya Shigenobu, Hideki Kaeriyama, and Takami Morita

**Abstract** We analyzed the contamination process by which the fat greenling, which was caught in the area off the mouth of the Ota River of Fukushima prefecture on August 1, 2012, concentrated radiocesium ( $^{134}\text{Cs} + ^{137}\text{Cs}$ ) to the level of 25,800 Bq/kg-wet. The radioactivity environment of the area was insufficient to maintain or increase the radiocesium concentration in the fish at the time. Distribution of the radioactive materials in the otolith of the fat greenling estimated by beta-ray emissions suggested that the fat greenling was in a highly contaminated environment during the period immediately following the Fukushima Dai-ichi Nuclear Power Plant (FNPP) accident. We used a biokinetic simulation of the  $^{137}\text{Cs}$  concentration to demonstrate that the fat greenling had to have been exposed to radioactivity from the FNPP to achieve such a high radiocesium concentration. Thus, the extremely contaminated fat greenling originated in the heavily contaminated environment of the FNPP port or the adjoining area in the period just after the accident.

**Keywords** Fat greenling • Contamination • Radiocesium • Autoradiography

### 13.1 Introduction

Radioactive nuclides leaked from the Fukushima Dai-ichi Nuclear Power Plant (FNPP), operated by Tokyo Electric Power Company (TEPCO), when it was damaged by the tsunami following the Tohoku Earthquake on March 11, 2011. The United Nations Scientific Committee on the Effects of Atomic Radiation

---

T. Watanabe (✉)

Tohoku National Fisheries Research Institute, Fisheries Research Agency,  
3-27-5, Shinhamma, Shiogama, Miyagi 985-0001, Japan  
e-mail: [wattom@affrc.go.jp](mailto:wattom@affrc.go.jp)

K. Fujimoto • Y. Shigenobu • H. Kaeriyama • T. Morita  
National Research Institute of Fisheries Sciences, Fisheries Research Agency,  
2-12-4, Fukuura, Kanazawa, Yokohama, Kanagawa 236-8648, Japan

© The Author(s) 2015

K. Nakata, H. Sugisaki (eds.), *Impacts of the Fukushima Nuclear Accident on Fish and Fishing Grounds*, DOI 10.1007/978-4-431-55537-7\_13

163

(UNSCEAR 2013) estimated the scale of the release of several radioactive nuclides: the range for radioactive iodine ( $^{131}\text{I}$ ) was from 100 to 500 petabecquerel (PBq) and the range for radiocesium ( $^{137}\text{Cs}$ ) was from 6 to 20 PBq. The committee noted that the amounts of released radioactive nuclides were much lower than that which occurred after the Chernobyl accident (the FNPP accident released 20 % of the  $^{137}\text{Cs}$  levels released after Chernobyl). The remarkable feature of the FNPP accident was the swift and direct release of highly polluted water to the ocean. Coastal area of Fukushima and adjacent prefectures were covered with seawater bearing high concentrations of  $^{131}\text{I}$  and radiocesium ( $^{134}\text{Cs}$  and  $^{137}\text{Cs}$ ) after the accident. The direct leakage of  $^{137}\text{Cs}$  was estimated as 3.5 PBq and the highest seawater concentration ( $>6 \times 10^4$  Bq/l) was observed at the coast near the FNPP (Tsumune et al. 2012). This value was seven orders of magnitude higher than the pre-accident levels.

The Ministry of Agriculture, Forestry and Fisheries (MAFF) and local government initiated emergency monitoring of radioactivity in marine products immediately after the accident to ensure food safety. Their findings were published on the websites of MAFF (2014) and of the Ministry of Health, Labor and Welfare (MHLW 2014). The Fisheries Research Agency (FRA) supported the measurement of radioactivity in marine products. In April 2011, extremely high levels of  $^{131}\text{I}$  and radiocesium ( $^{134}\text{Cs} + ^{137}\text{Cs}$ ;  $>1.0 \times 10^4$  Bq/kg-wet) were reported in sand lance larvae. Such high contamination levels were confined to larvae of pelagic fish in the area south of the FNPP and were thought to result from the spread of contaminated water after the accident (Tateda et al. 2013). After that,  $^{131}\text{I}$  contamination levels decreased rapidly, consistent with its short half-life (about 8.02 days), and returned to the levels below the limit of detection (hereinafter referred to as ND) after August 2011 (Wada et al. 2013). The relatively longer half-life of  $^{134}\text{Cs}$  (about 2.07 years) and  $^{137}\text{Cs}$  (about 30.1 years) caused them to remain in the marine environment for much longer; monitoring of radiocesium in the marine environment and marine products has continued.

Cesium is an alkali metal that is metabolized by the same pathway that metabolizes potassium, which is an essential mineral (Kaneko et al. 2013). As are other alkali metals, radiocesium is exchanged between the environment and body of marine teleost fish by their osmoregulatory systems, which maintain electrolyte balance (Evans 2010). Thus, radiocesium concentrations in the fish depend on the concentrations in the surrounding seawater. Wada et al. (2013) showed continuous reduction in radiocesium concentrations in marine products obtained off the coast of Fukushima Prefecture; the ecological half-life of radiocesium is much shorter than the physical half-lives of  $^{134}\text{Cs}$  and  $^{137}\text{Cs}$ .

TEPCO began to monitor radioactivity in marine fishes within a 20-km radius of FNPP (hereinafter referred to as the 20-km area) in March 2012. Against the decreasing trend of radiocesium in marine products, extremely high radiocesium concentrations were detected in *Hexagrammos otakii* (fat greenling) in the summer of 2012. The fat greenlings were caught about 1 km offshore near the mouth of the Ota River on August 1, 2012 (Chap. 12). The reported radiocesium ( $^{134}\text{Cs} + ^{137}\text{Cs}$ ) level was 25,800 Bq/kg-wet (TEPCO 2012a), the highest radiocesium concentration found in marine fishes at the time. An additional survey of fat greenlings in the area was conducted by TEPCO from September to October 2012, during which time 57 samples were examined (TEPCO 2012b). Most of the surveyed greenlings

showed radiocesium concentrations two orders of magnitude lower than that of the fat greenling caught in the area off the mouth of the Ota River on August 1, 2012. Radiocesium concentrations ranged from ND to 1,350 Bq/kg-wet (median, 77 Bq/kg-wet), equivalent to the levels found in samples taken outside the 20-km area. TEPCO's research on marine fish in the port of FNPP beginning in October 2012 showed highly contaminated fish species, including fat greenlings, with radiocesium concentrations exceeding 10,000 Bq/kg-wet (TEPCO 2014a). Statistical analysis of the data from fat greenlings showed that the probability of finding fat greenlings with  $^{137}\text{Cs}$  concentrations exceeding 16,000 Bq/kg-wet was below  $3.0 \times 10^{-6}$ , suggesting their radioactive exposure history was similar to that of the population in the port of FNPP (Shigenobu et al. 2014, Chap. 12).

The purpose of this study was to determine the contamination process of fat greenling by performing a quantitative analysis. We evaluated the radioactivity of the marine environment and the potential for generating highly contaminated fat greenlings. Analysis of fat greenling otoliths revealed the radioactive exposure history of the fish, the progress of which was examined by biokinetic model simulations.

### 13.2 $^{137}\text{Cs}$ Concentrations in Coastal Seawater and Marine Fish off the Coast of Fukushima Prefecture

Daily observed  $^{137}\text{Cs}$  concentrations in seawater sampled at TEPCO's monitoring stations around FNPP and the Fukushima Dai-ni Nuclear Power Plant (TEPCO 2014b) were used to evaluate radioactivity in the coastal areas of Fukushima Prefecture. Station locations are indicated in Fig. 13.1. The station at the shallow draft quay in the port of FNPP (hereinafter referred to as site-FP) was selected for the FNPP port; the northern side of the discharge channel for units 5–6 of FNPP (T-1) and the south discharge channel of FNPP, including stations T-2 and T-2-1, were selected to represent areas outside the FNPP port. The station at the north discharge channel of the Fukushima Dai-ni Nuclear Power Plant (T-3) and stations south thereof, around the Iwasawa shore (T-4), the north side of the Asami River (T-4-1), and the south side of the Kitasako River (T-4-2), were also chosen. To represent the average  $^{137}\text{Cs}$  concentration in the area outside the FNPP port (site-F1), data were averaged from T-1, T-2, and T-2-1. Averages were also generated for T-3, T-4, T-4-1, and T-4-2 to represent seawater around the Fukushima Dai-ni Nuclear Power Plant (site-F2). Thus, three daily time-series of  $^{137}\text{Cs}$  concentrations were generated for the period from March 21, 2011 to August 31, 2014. These values were used for the simulation of  $^{137}\text{Cs}$  concentrations in fat greenling.

Data points of ND were interpolated to produce continuous daily data. ND data during several days at site-FP were interpolated by using the minimum values obtained in the 15 days around the target day; longer consecutive ND periods were filled with values calculated from data obtained at other station in the port by regression analysis. ND data in the site-F1 and site-F2 time-series were filled in the same way.

Figure 13.2 shows the variations in seawater  $^{137}\text{Cs}$  concentration at the three sites. High  $^{137}\text{Cs}$  concentrations were simultaneously detected at all three stations

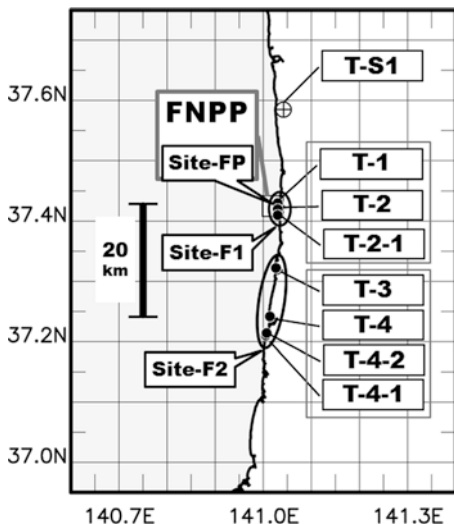


**Fig. 13.1** Locations of radiocesium monitoring stations along the coast of Fukushima prefecture. *Site-FP* represents the station at the shallow draft quay in the Fukushima Dai-ichi Nuclear Power Plant (FNPP) port. Stations T-1, T-2, and T-2-1 are adjacent to the FNPP port and are referred to as *site-F1*. Stations T-3, T-4, T-4-1, and T-4-2 are located around the Fukushima Dai-ichi Nuclear Power Plant and southward, referred to as *site-F2*. Station T-S1 is the collection point for the extremely contaminated fat greenling exhibiting 25,800 Bq/kg-wet radiocesium ( $^{134}\text{Cs} + ^{137}\text{Cs}$ )

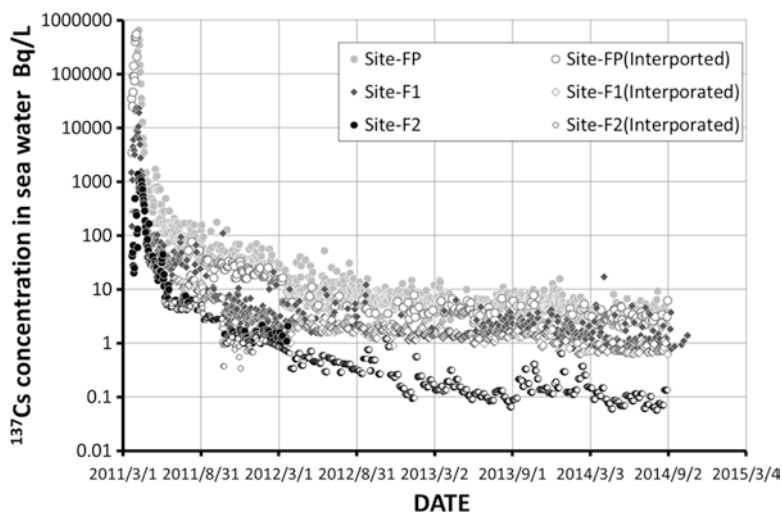


**Fig. 13.2** Combined time-series of observed and interpolated daily  $^{137}\text{Cs}$  concentration data at site-FP, site-F1, and site-F2 from March 21, 2011, to August 31, 2014

from late March to the beginning of April 2011. Peak values were  $6.6 \times 10^5$  Bq/l at site-FP,  $2.4 \times 10^4$  Bq/l at site-F1, and  $1.4 \times 10^3$  Bq/l at site-F2; values this high have never before been observed in the marine environment (Tsumune et al. 2012; Baxter and Camplin 1993; IAEA 2005; HELCOM 2009). Accumulated values for the period from March 21, 2011 to July 31, 2012, when the fat greenling was thought to be affected by contamination off the coast of Fukushima Prefecture, were as high as  $5.4 \times 10^6$  Bq/l at site-FP,  $2.2 \times 10^5$  Bq/l at site-F1, and  $1.8 \times 10^4$  Bq/l at site-F2. These accumulated values were indicative of the direct load of radioactivity in the ecosystem at each site. In addition, accumulation curves of  $^{137}\text{Cs}$  concentrations of each sites indicated sharp increase during the early days and reached 90 % of accumulated values of July 31, 2012 in first 20 (site-FP), 21 (site-F1), and 45 (site-F2) days.

$^{137}\text{Cs}$  concentration data for fat greenlings in the coastal waters of Fukushima Prefecture were extracted from the dataset published by MHLW (2014) and from TEPCO data reports for the 20-km area and the FNPP port (TEPCO 2014a). Time-series for fat greenlings in the coastal waters of Fukushima and for the 20-km area indicate similar decreasing trends beginning in the spring of 2012 (Fig. 13.3). The median and the 95th percentile values were calculated from the combined data set of both for each 6-month period beginning March 1, 2011. Ecological half-lives calculated from these values for the period from March 2012 to August 2014 were 175 days for 95th percentile and 194 days for median. The values were slightly lower than the results for fat greenlings (217 days) collected from the southern area off the coast of Fukushima Prefecture between August 2011 and September 2012 (Tateda et al. 2013). The difference reflected the variation in analytical period.

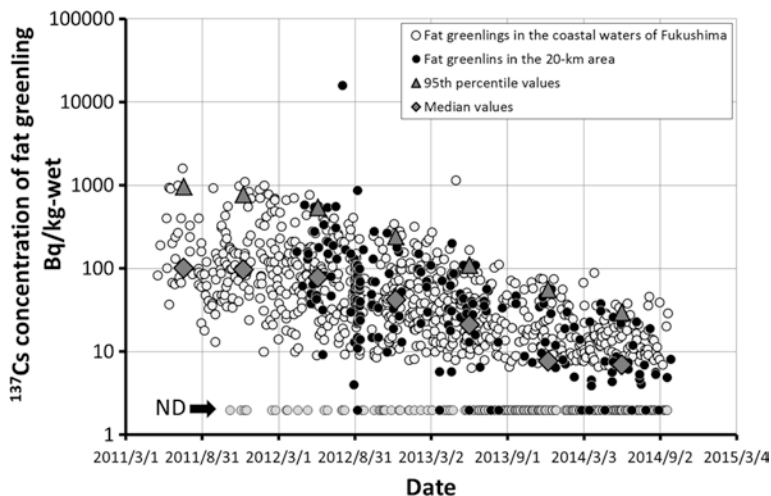


**Fig. 13.3** Temporal trends of observed  $^{137}\text{Cs}$  concentrations in fat greenlings caught in the coastal waters of Fukushima Prefecture, except the 20-km area and in the 20-km area with median values and 95th percentile values calculated from combined data of both for each 6-month period. The first term includes data from March 1, 2011 to August 31, 2011

### 13.3 The Marine Environment as a Source of Radioactive Contamination of the Fat Greenling

We sought to determine whether the observed radioactivity in the environment in the summer of 2012 could maintain radiocesium ( $^{134}\text{Cs} + ^{137}\text{Cs}$ ) concentrations of 25,800 Bq/kg-wet in the fat greenling. Marine fish obtain radiocesium from the environment via uptake of food and water.  $^{137}\text{Cs}$  concentrations in marine fish directly correlate with the concentrations in seawater under stable conditions (Kasamatsu 1999; IAEA 2004), expressed as the concentration factor (CF). Kasamatsu (1999) summarized the CFs of  $^{137}\text{Cs}$  for 27 species of marine teleost fish around Japan. The CFs were calculated from data obtained between 1984 and 1996; the average CF value for each fish species ranged from 22 to 122. The IAEA-recommended CF value of 100 for marine fish lies within this range (IAEA 2004). We estimated the CF for fat greenling off the coast of Fukushima prefecture from 29 measures obtained in 1982–2010, archived, and published by the NRA (Nuclear Regulation Authority 2014). The average CF was  $67 \pm 29$ , also within the range described by Kasamatsu (1999).

The CF value for fat greenling off the coast of Fukushima suggested that the surrounding seawater should contain  $^{137}\text{Cs}$  concentrations of 240 Bq/l to maintain a  $^{137}\text{Cs}$  concentration of 16,000 Bq/kg-wet (25,800 Bq/kg-wet for  $^{134}\text{Cs} + ^{137}\text{Cs}$ ) in the fish. In August 2012, the  $^{137}\text{Cs}$  concentration of seawater was less than 0.1 Bq/l off the coast of Fukushima Prefecture; the highest values observed in the FNPP port were also less than 100 Bq/l (TEPCO 2014b). TEPCO (2012b) also reported values much lower than 0.1 Bq/l in samples obtained around the Ota River.

We also considered the possibility that excretion of  $^{137}\text{Cs}$  from the fish was compensated for by ingestion of prey. Assuming a biological half-life of 100 days (World Health Organization and Food and Agriculture Organization of the United Nations 2011), the daily excretion rate was calculated as  $0.0069 \text{ day}^{-1}$  and the daily amount of  $^{137}\text{Cs}$  excreted from the fat greenling was 110 Bq/kg-wet. Assuming an ingestion rate of  $0.03 \text{ day}^{-1}$  and assimilation rate of 0.5 (Tateda 1997), the fat greenling would have to consume more than 7,300 Bq/kg-wet  $^{137}\text{Cs}$  daily to compensate for excretion. The  $^{137}\text{Cs}$  concentrations in the marine biota within the 20-km area were ND to 1,000 Bq/kg-wet (TEPCO 2014a), far below the required level.

Thus, the status of environmental  $^{137}\text{Cs}$  contamination in the area off the Ota River and in the 20-km area were insufficient to maintain the 16,000 Bq/kg-wet  $^{137}\text{Cs}$  concentration observed in the fat greenling, which were then assumed to be excreting excess radiocesium.

### 13.4 Radioactivity in the Otolith of Contaminated Fat Greenling

The fish otolith is a hard tissue that retains information on the age of the fish and the history of its environment, including temperature, salinity, and chemical composition (Campana 1999). The fish otolith consists mostly of calcium carbonate and

other elements that indicate environmental exposure. For example, strontium is often used as an indicator of environmental salinity (Tsukamoto et al. 1998). Radioactive materials absorbed in the otolith are also used as indicators of environmental conditions. Baker and Wilson (2001) showed that the otolith core of red snapper from the Gulf of Mexico contains  $^{14}\text{C}$  produced by nuclear testing. We analyzed the radioactive nuclides contained in the otolith of the fat greenling to characterize its history of radioactive exposure.

Contaminated fat greenling with radiocesium ( $^{134}\text{Cs} + ^{137}\text{Cs}$ ) concentrations of 25,800 Bq/kg-wet were caught from the area off the mouth of the Ota River and inspected for radioactivity by TEPCO, which provided the fish remnants from which the otoliths were extracted (Fig. 13.4). Radiation emitted from the otolith was measured with a germanium semiconductor detector for gamma-emitting nuclides and with a gas flow radiation counter for beta-emitting nuclides. Significant beta-ray emission was detected and gamma-ray emission was not detected (Fujimoto et al. 2013). Autoradiography was performed with imaging plates (IP) to visualize the distribution of radiation scatter from the sample materials.

We mounted a thin slice of the otolith on a glass slide and placed it on an IP (BAS-MS 2025; Fuji Film) for 13 days. The reaction strength to beta-ray emission

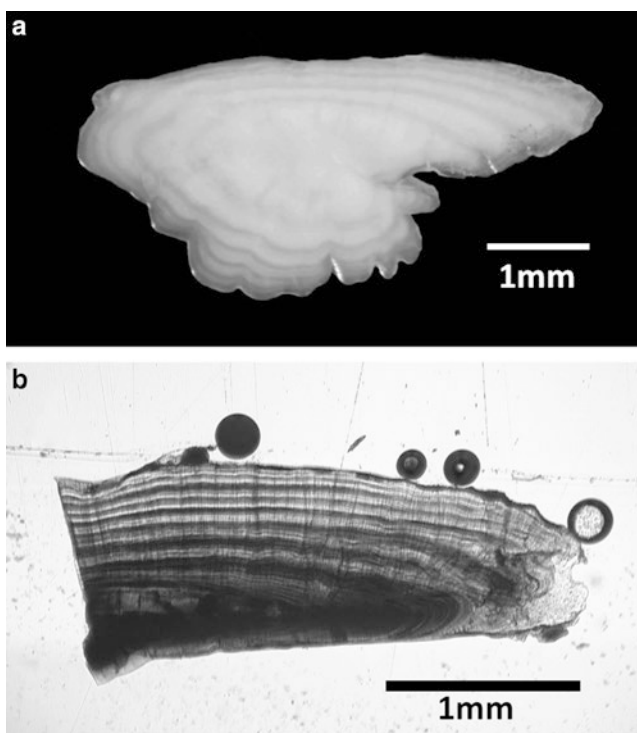


**Fig. 13.4** Otolith of the fat greenling (a) and its slice (b). The otolith in this figure was extracted from the *right side* of the fat greenling's head. The slice was cut from the *left-hand* otolith

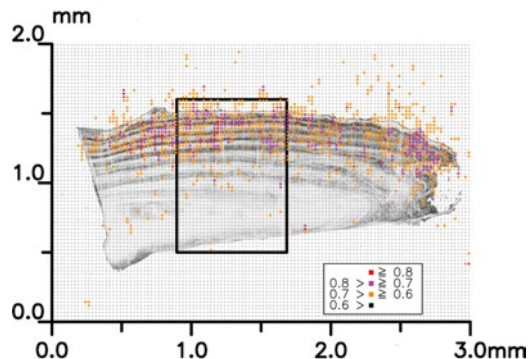


**Fig. 13.5** Image of the otolith slice and distribution of cumulative strength of incident radiation on an imaging plate (IP). Dense (*light*) shading areas of the otolith slice correspond to the transparent (opaque) zone. *Colors* indicate the cumulative strength normalized to the highest value. The *rectangle* encloses the area of detailed analysis where the zonal patterns of the annulus were obvious and the one-dimensional analysis along the *vertical* direction could be applied

was recorded on the IP and retrieved by an image analyzer (Typhoon 9400; GE Healthcare) with 25- $\mu\text{m}$  resolution. Beta rays were randomly emitted from the otolith and absorbed by the stimutable phosphor layer of the IP. The reaction strength reflects the accumulated number or energy of the beta rays. The distribution of the reaction strength on the IP was compared to digital images of the slice obtained by microscopy after careful justification of the pixel positions of both data. Figure 13.5 shows the distribution of reaction strength relative to the highest value on the image of the otolith slice. Higher reactions of the IP were observed around the area corresponding to the outer peripheral region of the slice. The relationship between the two images was quantified in the area indicated by the rectangle in Fig. 13.5, where the annulus had a clear zonal pattern and allowed one-dimensional analysis in the vertical direction. Thirty vertical rows of IP pixel data were included in the area. Relative reaction strength data in each vertical row were reconstructed by using the peak position of the second transparent zone as the origin. We compared the distribution of reaction strength detected by the IP with the vertical pattern consisting of opaque zones and transparent zones of the slice. The higher reaction of the IP corresponded to the area around the second transparent-opaque zone from outer edge of the slice (Fig. 13.6). We fitted a curve that had a form proportional to  $1/(h^2 + r^2)$  to the vertical distribution of the reaction strength.  $h$  is the distance from the otolith slice to the stimutable phosphor layer of the IP and  $r$  is the distance on the IP surface from the peak of the second transparent zone of the slice to each pixel position along the vertical axis. The formula approximated the distribution of incident radiation on a flat plane from a point source. The proportional coefficient and parameter  $h$  were estimated by the least-squares method using Solver in Excel. The statistical significance of the fitted curve in Fig. 13.6 was checked in a form of single regression analysis obtained by variable conversion. The fitted curve indirectly indicated that the position of the source of the radiation was located around the peak of the second transparent zone of the otolith slice. Considering an assumed error of



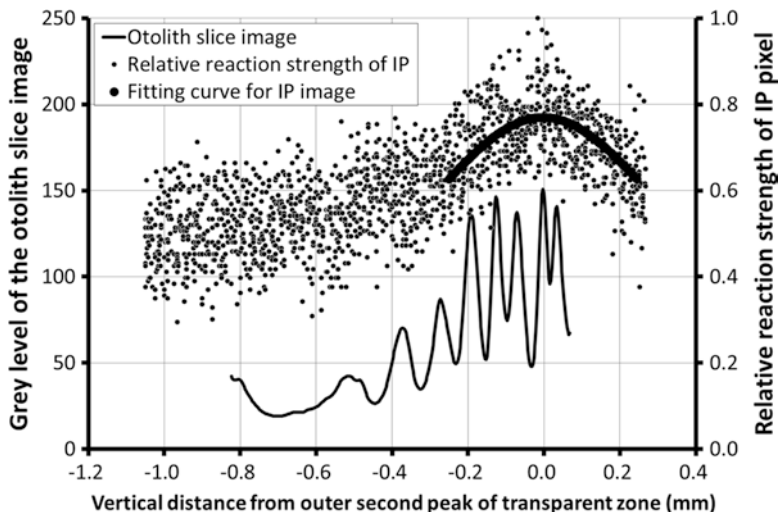


**Fig. 13.6** Comparison between the *grey level* of the otolith slice and the relative reaction strength of the IP for the enclosed area in Fig. 13.5. Thirty *vertical rows* of IP pixel data were included. Relative reaction strength data for each *vertical row* were reconstructed by using the peak position of the second transparent zone as the origin. The *vertical* distribution of the zonally averaged *grey level* of the otolith slice is shown by a *solid thin line*. Lower (higher) *grey levels* in the otolith slice correspond to the opaque (transparent) zone. The relative reaction strength of each pixel of the IP is shown with a *full circle*. The *fitted curve* for the IP pixel data in the area around the peak of the second transparent zone is shown by a sequence of *large full circles*. *Upward arrow* indicates the center of the second transparent zone

$\pm 1$  pixel ( $0.025 \mu\text{m}$ ) in justifying the slice and IP images, the probability of containing more radioactive materials was high in the area from the second to the third opaque zones of the otolith slice.

The opaque zone of the otolith was formed in the summer season (Sekigawa et al. 2002); the first transparent-opaque zone on the slice from the fat greenling caught in the summer of 2012 was thought to correspond to the period from autumn 2011 to summer 2012. Thus, the second zone containing the most beta ray-emitting radionuclides corresponded to the period from autumn 2010 to summer 2011. These results strongly suggested that the fat greenling was in an environment rich in beta ray-emitting nuclides between the spring and summer of 2011.

A possible candidate of beta ray-emitting radionuclide contained in the otolith was  $^{90}\text{Sr}$ . The beta-ray emissions from the otolith of several fish species collected in the FNPP port were associated with  $^{90}\text{Sr}$  concentration in the body, excluding the viscera, and were associated with  $^{137}\text{Cs}$  in the muscle tissue (Fujimoto et al. 2013). The amount of  $^{90}\text{Sr}$  leakage was estimated at about 3 % of  $^{137}\text{Cs}$  (Casacuberta et al. 2012), but it was thought that the  $^{90}\text{Sr}$  concentration in seawater rapidly increased, similar to  $^{137}\text{Cs}$  from late March to the beginning of April 2011. From these relationships, we hypothesized that the fat greenling absorbed a large amount of radioactive nuclides in the period just after the FNPP accident when contaminated seawater covered the coastal area of Fukushima Prefecture.

### 13.5 Simulation of $^{137}\text{Cs}$ Concentrations in Fat Greenlings Using a Biokinetic Model

To test our hypothesis, we simulated the contamination of fat greenling in a biokinetic model of  $^{137}\text{Cs}$  exchange between environment and biota. Many types of biokinetic model have been used to simulate the concentration of radioactive nuclides in fish (Brown et al. 2006; Kanish and Aust 2013; Tateda et al. 2013). We constructed a simple model of two compartments as shown by Brown et al. (2006). The equation for  $^{137}\text{Cs}$  concentration in a fat greenling is expressed as Eq. (13.1). The  $^{137}\text{Cs}$  concentrations in marine fish are mediated by uptake through drinking seawater (first term), ingestion of prey (second term), and excretion by the osmoregulation system (last term). Explanations for each variable and parameter are given in Table 13.1. Most values were set according to Tateda (1997). As the fat greenling is thought to be omnivorous (Kasamatsu 1999), we set the  $^{137}\text{Cs}$  concentration of prey as a mixture of two groups of marine biota: one group was fish and the other was invertebrates. The  $^{137}\text{Cs}$  concentration in prey fish was determined by Eq. (13.1). The  $^{137}\text{Cs}$  concentrations in invertebrates were calculated by Eq. (13.2), in which uptake of  $^{137}\text{Cs}$  is directly related to the seawater concentration of  $^{137}\text{Cs}$ . The parameters of  $k_{pi}$  and  $CF_{pi}$  empirically determined that the predicted  $^{137}\text{Cs}$  values by Eq. (13.2) followed the observed  $^{137}\text{Cs}$  values for invertebrates off Fukushima Prefecture. After determining the parameters in Eq. 13.2, we tuned the mixture rate of the prey groups to obtain a simulated CF of fat greenling in the range of 60–70 by using the constant  $^{137}\text{Cs}$  concentration value. In addition, the effect of physical disintegration of  $^{137}\text{Cs}$  was discarded because it has a 100-fold-longer half-life (about 30.1 years) in comparison to the biological half-life (about 100 days):

**Table 13.1** Variables and parameters in the biokinetic equation for a fat greenling

| Variable  | Value               | Unit                     | Explanation                                               |
|-----------|---------------------|--------------------------|-----------------------------------------------------------|
| $C_f$     |                     | Bq/kg-wet                | $^{137}\text{Cs}$ concentration in fish body              |
| $C_{pf}$  |                     | Bq/kg-wet                | $^{137}\text{Cs}$ concentration in prey fish body         |
| $C_w$     |                     | Bq/l                     | $^{137}\text{Cs}$ concentration of surrounding seawater   |
| $C_{pi}$  |                     | Bq/kg-wet                | $^{137}\text{Cs}$ concentration of prey invertebrate      |
| $k_w$     | 0.10 <sup>a</sup>   | (kg/l) day <sup>-1</sup> | Uptake rate of $^{137}\text{Cs}$ activity from seawater   |
| $IR_f$    | 0.030 <sup>a</sup>  | day <sup>-1</sup>        | Ingestion rate per unit mass of fish                      |
| $AE_f$    | 0.50 <sup>a</sup>   | No dimension             | Assimilation efficiency for fish                          |
| $k_f$     | 0.0088 <sup>a</sup> | day <sup>-1</sup>        | Excretion rate of $^{137}\text{Cs}$ for fish              |
| $CF_{pi}$ | 10 <sup>b</sup>     | No dimension             | Concentration factor for prey invertebrate                |
| $k_{pi}$  | 0.0087 <sup>b</sup> | day <sup>-1</sup>        | Excretion rate of $^{137}\text{Cs}$ for prey invertebrate |
| $a$       | 0.36 <sup>b</sup>   | No dimension             | Mixing ratio of prey fish                                 |

<sup>a</sup>Values were adopted from Tateda (1997)

<sup>b</sup>Values were experimentally determined in this study

$$\frac{dC_f(t)}{dt} = k_w \cdot C_w(t) + IR_f \cdot AE_f \cdot [a \cdot C_{pf}(t) + (1-a) \cdot C_{pi}(t)] - k_f \cdot C_f(t) \tag{13.1}$$

$$\frac{dC_{pi}(t)}{dt} = CF_{pi} \cdot k_{pi} \cdot C_w(t) - k_{pi} \cdot C_{pi}(t) \tag{13.2}$$

The time course of <sup>137</sup>Cs accumulation in the fat greenlings was simulated by using the <sup>137</sup>Cs concentration data from seawater at site-FP, site-F1, and site-F2 (shown in Fig. 13.7 with observed data). The derivation curve of <sup>137</sup>Cs concentrations for site-F2 (thick solid line) was a good approximation of the envelope curve of observation data. The <sup>137</sup>Cs concentration of fat greenling at site-F2 reached maximum in mid-July 2011, then decreased. The simulated ecological half-life for the period after March 2012 is about 208 days, similar to the values calculated from observed data (13.2). An evaluation of the contribution of each term in Eq. (13.1) showed that uptake of <sup>137</sup>Cs from the seawater was largely responsible for the increasing <sup>137</sup>Cs concentration in the first month, during which time the concentration increased to 80 % of the maximum value. After this point, low but steady uptake via prey contributed to a slow increase toward the maximum <sup>137</sup>Cs concentration in mid-July and the slow decrease thereafter. These features are identical to the simulation results for coastal fish indicated by Tateda et al. (2013). We conclude that the simplified model is appropriate for simulating <sup>137</sup>Cs concentrations in fat greenling off the coast of Fukushima.

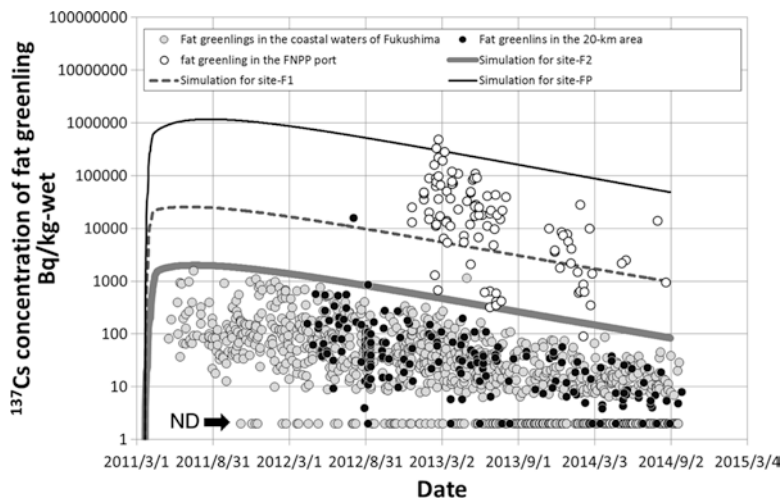


**Fig. 13.7** Simulated <sup>137</sup>Cs concentration of fat greenlings for site-FP, site-F1, and site-F2 with observed <sup>137</sup>Cs concentrations in fat greenling caught in the coastal waters of Fukushima Prefecture, except the 20-km area, in the 20-km area, and in the FNPP port

Simulation results for site-F1 (dashed line) and site-FP (thin solid line) are also shown in Fig. 13.7. The same curve shape was observed, although at a different level. Maximum  $^{137}\text{Cs}$  concentration were observed in mid-July and correlated with the integrated values in seawater. The observed  $^{137}\text{Cs}$  concentration in fat greenling from the FNPP port was moderately simulated by the model. The  $^{137}\text{Cs}$  concentration in the highly contaminated fat greenling was in the range between simulations for site-FP in the FNPP port and site-F1. These model simulations support the hypothesis that the fat greenling collected in the summer of 2012 off the mouth of the Ota River had been exposed to the highly contaminated environment in the FNPP port or adjoining areas.

The range of  $^{137}\text{Cs}$  concentrations formed by the large difference between simulations for site-FP and site-F1 bracketed the majority of the distribution of  $^{137}\text{Cs}$  concentrations in fat greenlings in the FNPP port. The  $^{137}\text{Cs}$  concentration data at site-FP were within the intermediate range compared with other observation points at the initial stage of the radiation leak. Available seawater  $^{137}\text{Cs}$  concentration data from April 2011 showed that the averaged value for the observation point in the intake canal south of site-FP was several times higher than the value at site-FP. The minimum values of  $^{137}\text{Cs}$  concentrations in the port, where the concentrations were probably no lower than the level found outside the port (site-F1), where the concentration was about one order of magnitude lower than at site-FP. The large variability of observed  $^{137}\text{Cs}$  concentrations in fat greenling was partly attributed to the local spatial and temporal distribution of  $^{137}\text{Cs}$  in the FNPP port. In additional simulations of a fat greenling entering the FNPP port after the peak period of environmental contamination, highly contaminated fat greenlings were also generated, mainly by prey uptake. This process might also maintain the wider range in the group of highly contaminated fat greenlings in the FNPP port.

As for the extremely contaminated fat greenling caught in the area off the mouth of the Ota River, radioactivity in the otolith and the simulation suggested a generation scenario. The fat greenling were living in the FNPP port or in the adjoining area when contaminated water leaked to the sea and highly contaminated seawater covered the area. The  $^{137}\text{Cs}$  concentration of the fat greenling may have reached about 100,000 Bq/kg-wet. The relatively lower concentration compared with other fat greenlings in the FNPP port suggest the habitat was apart from the intake canal of the FNPP port and the fat greenling was able to avoid a direct encounter with the more highly contaminated seawater. After the direct leakage of highly contaminated water to the sea, the fat greenling eventually left the port.

**Acknowledgments** The authors appreciate the members of the Research Center for Fisheries Oceanography and Marine Ecosystem of the National Research Institute of Fisheries Science for their support. The sliced sample of the otolith was processed by Japan NUS, and the autoradiographic measurement of the otolith slice was performed by BayBioImaging. This study was financially supported by the Fisheries Agency.

**Open Access** This chapter is distributed under the terms of the Creative Commons Attribution Noncommercial License, which permits any noncommercial use, distribution, and reproduction in any medium, provided the original author(s) and source are credited.

## References

- Baker MS Jr, Wilson CA (2001) Use of bomb radiocarbon to validate otolith section ages of red snapper *Lutjanus campechanus* from the northern Gulf of Mexico. *Limnol Oceanogr* 46:1819–1824
- Baxter AJ, Camplin WC (1993) Measures of dispersion from discharge pipelines at nuclear sites in the UK using caesium-137 in sea water data. Fisheries research data report no. 34. Ministry of Agriculture, Fisheries and Food, Directorate of Fisheries Research, Lowestoft
- Brown J, Dowdall M, Gwynn JP, Børretzen P, Selnaes ØG, Kovacs KM, Lydersen C (2006) Probabilistic biokinetic modelling of radiocaesium uptake in Arctic seal species: verification of modelled data with empirical observations. *J Environ Radioact* 88:289–305
- Campana SE (1999) Chemistry and composition of fish otolith: pathways, mechanisms and applications. *Mar Ecol Prog Ser* 188:263–297
- Casacuberta N, Masqué P, Garcia-Orellana J, Garcia-Tenorio R, Buesseler KO (2012) <sup>90</sup>Sr and <sup>89</sup>Sr in seawater off Japan as a consequence of the Fukushima Dai-ichi nuclear accident. *Biogeosciences* 10:3649–3659
- Evans DH (2010) A brief history of the study of fish osmoregulation: the central role of the Mt. Desert Island Biological Laboratory. *Front Physiol* 1:13
- Fujimoto K, Miki S, Kaeriyama H, Shigenobu Y, Takagi K, Ambe D, Ono T, Watanabe T, Morinaga K, Nakata K, and Morita T (2013) Levels of radioactive cesium contamination in three fish species caught in the main harbor of Fukushima Dai-ichi Nuclear Power Plant, and a trial to estimate strontium-90 from fish otoliths. (submitted to *Environ Sci Technol*)
- HELCOM (2009) Radioactivity in the Baltic Sea, 1999-2006: HELCOM thematic assessment. Baltic Sea environment proceedings no. 117. HELCOM, Helsinki
- IAEA (2004) Sediment distribution coefficients and concentration factors for biota in the marine environment. Technical reports series no. 422. IAEA, Vienna
- IAEA (2005) Worldwide marine radioactivity studies (WOMARS): radionuclide levels in oceans and seas. IAEA-TECDOC-1429. IAEA, Vienna
- Kaneko T, Furukawa F, Watanabe S (2013) Excretion of cesium through potassium transport pathway in the gills of a marine teleost. In: Nakanishi TM, Tanoi K (eds) *Agricultural implications of the Fukushima nuclear accident*. Springer Japan, Tokyo
- Kanish G, Aust M-O (2013) Does the Fukushima NPP disaster affect the caesium activity of North Atlantic Ocean fish? *Biogeosciences* 10:5399–5410
- Kasamatsu F (1999) Marine organisms and radionuclides with special reference to the factors affecting concentrations of <sup>137</sup>Cs in marine fish. *Radioisotopes* 48:266–282 (in Japanese)
- MAFF (2014) Results of the monitoring on radioactivity level in fisheries products. <http://www.jfa.maff.go.jp/e/inspection/index.html>. Date of access: 11 Nov 2014
- MHLW (2014) Levels of radioactive contaminants in foods tested in respective prefectures. [http://www.mhlw.go.jp/english/topics/2011eq/index\\_food\\_radioactive.html](http://www.mhlw.go.jp/english/topics/2011eq/index_food_radioactive.html). Date of access: 11 Nov 2014
- NRA (2014) Environmental radioactivity and radiation in Japan (in Japanese). <http://www.kankyo-hoshano.go.jp/>. Date of access: 11 Nov 2014
- Sekigawa T, Takahashi T, Takatsu T (2002) Age and growth of fat greenling *Hexagrammos otakii* in Kikonai Bay, Hokkaido. *Aquat Sci* 50:395–400 (in Japanese)
- Shigenobu Y, Fujimoto K, Ambe D, Kaeriyama H, Ono T, Morinaga K, Nakata K, Morita T, Watanabe T (2014) Radiocesium contamination of greenlings (*Hexagrammos otakii*) off the coast of Fukushima. *Sci Rep* 4:6851
- Tateda Y (1997) Basic model for the prediction of <sup>137</sup>Cs concentration in the organisms of detritus food chain. Abiko Research Laboratory CRIEPI report no. 94056. CRIEPI, Chiba (in Japanese)
- Tateda Y, Tsumune D, Tsubono T (2013) Simulation of radioactive cesium transfer in the southern Fukushima coastal biota using a dynamic food chain transfer model. *J Environ Radioact* 124:1–12
- TEPCO (2012a) High cesium density detected in greenling. [http://www.tepco.co.jp/en/nu/fukushima-np/images/handouts\\_120828\\_02-e.pdf](http://www.tepco.co.jp/en/nu/fukushima-np/images/handouts_120828_02-e.pdf). Date of access: 11 Nov 2014

- TEPCO (2012b) Additional survey on high-caesium-level greenling and future countermeasures. [http://www.tepco.co.jp/en/nu/fukushima-np/images/handouts\\_121126\\_03-e.pdf](http://www.tepco.co.jp/en/nu/fukushima-np/images/handouts_121126_03-e.pdf). Date of access: 11 Nov 2014
- TEPCO (2014a) Analysis results of fish and shellfish (The Ocean Area Within 20-km Radius of Fukushima Daiichi NPS). <http://www.tepco.co.jp/en/nu/fukushima-np/f1/smp/index-e.html>. Date of access: 21 Nov 2014
- TEPCO (2014b) Result of radioactive nuclide analysis for the seawater sampled onshore and offshore of the power station. <http://www.tepco.co.jp/en/nu/fukushima-np/f1/smp/2014/images/seawater-newest01-e.csv>. Date of access: 21 Nov 2014
- Tsukamoto K, Nakai I, Tesch W-V (1998) Do all freshwater eels migrate? *Nature (Lond)* 396:635–636
- Tsumune D, Tsubono T, Aoyama M, Hirose K (2012) Distribution of oceanic  $^{137}\text{Cs}$  from the Fukushima Daiichi Nuclear Power Plant simulated numerically by a regional ocean model. *J Environ Radioact* 111:100–108
- UNSCEAR (2013) Sources, effects and risks of ionizing radiation (Report to the General Assembly). UNSCEAR, New York
- Wada T, Nemoto Y, Shimamura S, Fujita T, Mizuno T, Sohtaome T, Kamiyama K, Morita T, Igarashi S (2013) Effects of the nuclear disaster on marine products in Fukushima. *J Environ Radioact* 124:246–254
- World Health Organization and Food and Agriculture Organization of the United Nations (2011) Impact on seafood safety of the nuclear accident in Japan. <http://www.iaea.org/newscenter/focus/fukushima/seafoodsafety0511.pdf>